International Journal of Solids and Structures 49 (2012) 1764–1772

Contents lists available at SciVerse ScienceDirect

International Journal of Solids and Structures

journal homepage: www.elsevier.com/locate/ijsolstr

Solution for dissimilar elastic inclusions in a finite plate using boundary integral equation method

Y.Z. Chen *

Division of Engineering Mechanics, Jiangsu University, Zhenjiang, Jiangsu 212013, PR China

ARTICLE INFO

Article history:
Received 7 November 2011
Received in revised form 15 March 2012
Available online 24 March 2012

Keywords:
Complex variable boundary integral equation
Inverse matrix technique
Inclusion problem
Stress concentration
Composite Materials

ABSTRACT

This paper studies the boundary value problem for a finite plate containing two dissimilar inclusions. The matrix and the two inclusions have different elastic properties. The loadings applied along the outer boundary are in equilibrium. The mentioned problem is decomposed into three boundary value problems (BVPs). Two of them are interior BVP for the elastic inclusions, while the other is a BVP for the triply-connected region. Three problems are connected together through the common displacements and tractions along the interface boundaries. Explicit form for the complex variable boundary integral equation (CVBIE) is derived. After discretization of relevant BIEs, the solutions are evaluated numerically. Three numerical examples for different elastic constant combinations are provided.

1. Introduction

In earlier years, some pioneer researchers studied and developed the boundary integral equation (abbreviated as BIE) in elasticity and some relevant topics (Rizzo, 1967; Cruse, 1969; Jaswon and Symm, 1977; Brebbia et al., 1984; Hong and Chen, 1988). An article reviewed the early history of the boundary element method up to the late 1970s (Cheng and Cheng, 2005).

It is a rare case that those BIEs can be solved in a closed form. After discretization for the BIE along the boundaries, the relevant boundary element method (abbreviated as BEM) is thus formulated. A particular advantage of the BEM is that the numerical discretization is conducted at a reduced spatial dimension. In the BEM formulation, there is no need of dealing with the interior mesh. Therefore, the BEM is more effective in the mesh preparation.

The composites are widely used in industry nowadays. Generally, the composites may contain some inclusions, which have different elastic properties with the matrix medium. The stress distribution in the composites may not be uniform. Particularly, if the inclusion is softer, the stress concentration must exist along the interface boundary at the matrix side. Therefore, it is an important problem to investigate the stress distribution in the medium with the dissimilar elastic inclusions. Because of its importance in elasticity many researchers attracted this problem.

Based on the conformal mapping functions, some problems for the elastic medium with dissimilar inclusions were solved by Chang and Conway (1969), Luo and Gao (2009). The used technique relies on the conformal mapping closely, and it is not easy to develop the suggested technique to the arbitrary configuration for the embedded inclusions. Solution for the problem of an isotropic elastic half-plane containing many circular elastic inclusions was proposed, where the complex-variable hypersingular integral equation was used (Legros et al., 2004). The obtained solution was for the case of circular inclusion.

A boundary-domain integral equation in elastic inclusion problems was introduced by Dong et al., (2002). In the formulation, the inclusion portion is assumed in a discrete form, and the strain components in the inclusion were unknowns. In addition, some integral equation approaches were used to solve some particular problems with involved inclusions (Dong et al., 2004; Dong and Lee, 2005).

Based on the body force method, a singular integral equation method for interaction between elliptical inclusions was suggested by Noda and Matsuo (1998). The problem is formulated as a system of singular integral equations with Cauchy-type or logarithmic-type singularities, where the unknowns are the body force densities. As an extension, the method was used to a similar problem in the longitudinal shear loading (Noda and Matsuo, 2000). Those solutions are suitable and effective to solve the inclusion problem with elliptical configuration.

A null-field integral equation was derived. The equation was used for an infinite medium containing circular holes and/or

* Tel.: +86 511 88780780.
E-mail address: chens@ujs.edu.cn

0020-7683/$ - see front matter © 2012 Elsevier Ltd. All rights reserved.
http://dx.doi.org/10.1016/j.ijsolstr.2012.03.021

inclusions with arbitrary radii and positions under the remote antiplane shear (Chen and Wu, 2007; Chen and Li, 2009). By using the collocation method, the null-field integral equation becomes a set of algebraic equations for the Fourier coefficients.

It is seen from the motioned references that the inclusion problems have not been solved very well previously. For example, some solutions depend on the conformal mapping function, and they are not derived from an arbitrary configuration of inclusion. Here we only cite a portion of references for the inclusion problems, and may lose some publications in this field.

A complex variable boundary integral equation (CVBIE) for plane elasticity was suggested by Chen and Lin (2010). However, the paper only proposed basic governing equations for the interior and the exterior boundary value problems (BVPs). Those equations are not sufficient to solve the problem of dissimilar inclusions studied below.

This paper studies the boundary value problem for a finite plate containing two dissimilar inclusions. The matrix and the two inclusions have different elastic properties. The loadings applied along the outer boundary are in equilibrium. The mentioned problem is decomposed into three BVPs. Two of them are an interior BVP for the elastic inclusions, while the other is a BVP for the triply-connected region. Three problems are connected together through the common displacements and tractions along the interface boundaries. Explicit forms for the CVBIE is derived.

In the original formulation, the tractions along the interfaces of matrix and the inclusions are two unknowns. After the discretization of BIEs, a numerical solution technique is suggested. In the technique, an inverse matrix technique is suggested which can eliminate the two unknown vectors in advance. This can considerably reduce the work for assembling the matrices and the size of resulting matrix. Three numerical examples for different elastic constant combinations are provided. From a wide range of the ratio for the two shear moduli of elasticity changing from near 0 (10^{-5}), 0.1, 0.5 1,2 to 10, it is found that the stress distributions in the matrix and inclusions are rather complicated.

2. Analysis

Analysis presented below mainly depends on two forms of integral equation. Among them, one is used for a single-connected region, and the other is used for a multiply-connected region. After linking two kinds of the integral equation together, the solution for dissimilar elastic inclusions in a finite plate is obtainable.

2.1. Complex variable boundary integral equations (CVBIE) for interior region and multiply-connected region

There are two kinds of formulation for the BIE in plane elasticity. Among them, one is based on the real variable (Rizzo, 1967; Cruse, 1969; Jaswon and Symm, 1977; Brebbia et al., 1984; Hong and Chen, 1988; Cheng and Cheng, 2005). However, it is more straightforward to formulate the BIE with the usage of the complex variable. In the complex variable boundary integral equations (CVBIE), all involved kernels are expressed in an explicit form. Therefore, the singular portion in the kernels of CVBIE is easy to distinguish. Some relevant formulations based on complex variable can be referred to (Kolte et al., 1996; Mogilevskaya and Linkov, 1998; Mogilevskaya, 2000; Chen and Chen, 2000; Chen et al., 2002; Linkov, 2002; Chen and Wang, 2010).

In the present study, one needs to propose two forms of CVBIE. One is used for a single-connected region, and the other is used for a multiply-connected region.

For the single-connected region (Fig. 1), a CVBIE for the interior problem is introduced below (Chen and Lin, 2010)

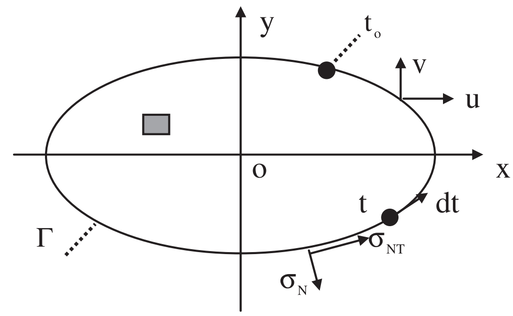

Fig. 1. Interior boundary value problem, (▭) region defined.

$$\frac{U(t_o)}{2} + B_1 \mathrm{i}\int_\Gamma \left(\frac{\kappa-1}{t-t_o}U(t)\mathrm{d}t - \mathrm{L}_1(t,t_o)U(t)\mathrm{d}t + \mathrm{L}_2(t,t_o)\overline{U(t)}\mathrm{d}t\right)$$
$$= B_2\mathrm{i}\int_\Gamma \left(2\kappa\ln|t-t_o|\mathrm{Q}(t)\mathrm{d}t + \frac{t-t_o}{\bar{t}-\bar{t}_o}\overline{\mathrm{Q}(t)}\mathrm{d}\bar{t}\right) \quad (t_o \in \Gamma), \quad (1)$$

where Γ denotes the boundary of the interior region and the increase "dt" is defined in the anti-clockwise direction. Generally, the increase "dt" takes a complex value, which is indicated in Fig. 1. In addition, $d\bar{t}$ is a conjugate value with respect to the increase "dt". In Eq. (1), $U(t)$ and $Q(t)$ denote the displacement and traction along the boundary Γ, which are defined by

$$U(t) = u(t) + iv(t), \quad Q(t) = \sigma_N(t) + i\sigma_{NT}(t) \quad (t \in \Gamma). \quad (2)$$

In Eq. (2), $u(t)$ and $v(t)$ take the real value and $U(t) = u(t) + iv(t)$ is a complex value. Similarly, $\sigma_N(t)$ and $\sigma_{NT}(t)$ take the real value and $Q(t) = \sigma_N(t) + i\sigma_{NT}(t)$ is a complex value. Those notations have been indicated in Fig. 1.

In addition, two elastic constants and two kernels are defined by

$$B_1 = \frac{1}{2\pi(\kappa+1)}, \quad B_2 = \frac{1}{4\pi G(\kappa+1)} \quad (3)$$

$$L_1(t,\tau) = -\frac{\mathrm{d}}{\mathrm{d}t}\left\{\ln\frac{t-\tau}{\bar{t}-\bar{\tau}}\right\} = -\frac{1}{t-\tau} + \frac{1}{\bar{t}-\bar{\tau}}\frac{\mathrm{d}\bar{t}}{\mathrm{d}t},$$
$$L_2(t,\tau) = \frac{\mathrm{d}}{\mathrm{d}t}\left\{\frac{t-\tau}{\bar{t}-\bar{\tau}}\right\} = \frac{1}{\bar{t}-\bar{\tau}} - \frac{t-\tau}{(\bar{t}-\bar{\tau})^2}\frac{\mathrm{d}\bar{t}}{\mathrm{d}t} \quad (4)$$

where $\kappa = 3 - 4v$ (for plane strain condition), $\kappa = (3 - v)/(1 + v)$ (for plane stress condition), G is the shear modulus of elasticity, and v is the Poisson's ratio. In this paper, the plane strain condition and $v = 0.3$ are assumed. In Eq. (4), τ denotes a domain point or a point on the boundary.

Similarly, the relevant BIE can be formulated for the multiply-connected region (Fig. 2). Without losing generality, we consider triply-connected region only. In this case, from a modification to Eq. (1), the relevant BIE will be

$$\frac{U_j(t_o)}{2} + B_1 i\sum_{k=1}^{3}\int_{\Gamma_k}\left(\frac{\kappa-1}{t-t_o}U_k(t)\mathrm{d}t - L_1(t,t_o)U_k(t)\mathrm{d}t + L_2(t,t_o)\overline{U_k(t)}\mathrm{d}t\right)$$
$$= B_2 i\sum_{k=1}^{3}\int_{\Gamma_k}\left(2\kappa\ln|t-t_o|Q_k(t)\mathrm{d}t + \frac{t-t_o}{\bar{t}-\bar{t}_o}\overline{Q_k(t)}d\bar{t}\right)$$
$$(t_o \in \Gamma_j, j = 1,2,3) \quad (5)$$

where the kernels have been defined previously. In Eq. (5) or Fig. 2, if one goes forward with the increase "dt", the considered medium must be at the left hand side. That is to say for the outer boundary Γ_3, the integration path "dt" should be in the anti-clockwise direction, and for the inner boundaries Γ_1 and Γ_2 in clockwise direction (Fig. 2). In addition, it is noted for Eq. (5) that only for $t_o \in \Gamma_j$, and the integration "dt" along the same Γ_j ($j = 1, 2, 3$), there are singular kernel $1/(t - t_o)$ or weaker singular kernel $\ln|t - t_o|$.

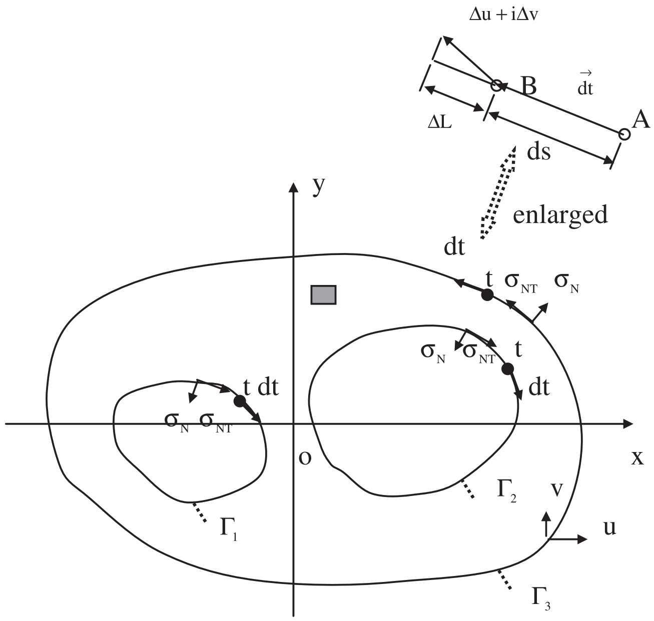

Fig. 2. Boundary value problem for triply-connected region, (▭) region defined.

Some differences between the complex variable BIE and the real variable BIE may be found in some aspects. First of all, there is a difference for operator defined in the right hand of Eq. (1) (Chen et al., 2009; Chen and Lin, 2010). Those operators, or the kernel functions, have a difference of constants in the different formulations (Chen et al., 2009). If the loadings on the contour in an exterior BVP are not in equilibrium, the regularity condition at infinity shown by (Brebbia et al., 1984, Eq. (5.82)) is not satisfied by the relevant operator in the real variable formulation (Chen et al., 2009). However, in the same condition, the regularity condition at infinity is satisfied by the relevant operator in the complex variable formulation.

Secondly, the properties of some kernel functions in the complex variable formulation are easy to recognize. For example, it is assumed that we perform integration along a line element on the boundary. If we denote $t = se^{i\gamma}$ ($dt = e^{i\gamma}ds$) and $t_o = s_o e^{i\gamma}$, and we can find $L_1(t, t_o) = 0$ defined by Eq. (4) immediately.

In addition, it is slightly easier to formulate the program if one uses the kernels based on the complex variable formulation. For example, in the discretization for the left hand side of Eq. (1), we simply put $U(t) = 1$ or $U(t) = i$, and separate the real and the imaginary portions and the influence matrix will be formulated immediately.

Simply because the loadings on contour are in equilibrium in the present study, the computed results must be the same from two kinds of formulation.

2.2. Formulation for the problem of two dissimilar inclusions in a finite plate

The original problem for a finite plate with two dissimilar elastic inclusions is shown by Fig. 3(o), where the loading σ_N, σ_{NT} are applied along the outer boundary Γ_3. Those loadings must be in equilibrium. The dissimilar inclusions may have different shapes. In addition, the dissimilar inclusions are defined such that one or two of the elastic constants are different. The matrix medium in finite plate bounded by contours Γ_1, Γ_2 and Γ_3 has the elastic constants (G_3, ν_3), where G_3, ν_3 denote the shear modulus of elasticity and Poisson's ratio, respectively. Two inclusions have the elastic constants (G_1, ν_1) and (G_2, ν_2), respectively. The problem can be decomposed into three problem shown by Fig. 3(a), (b) and (c), respectively.

The problem shown by Fig. 3(a) is devoted to an interior boundary value problem with the outer boundary Γ_1 and the elastic constants (G_1, ν_1). The applied displacement and the traction along the boundary Γ_1 are denoted by $\{u_1\}$ and $\{q_1\}$, respectively. Generally, the boundary integral equation is solved numerically in a discrete form. In this case, $\{u_1\}$ is a vector composed of many "u" and "v" components at many discrete points, which is expressed as

$$\{u_1\} = \{u_{*1} \;\; v_{*1} \;\; \cdots \;\; u_{*j} \;\; v_{*j} \;\; \cdots \;\; u_{*M} \;\; v_{*M}\}^T \tag{6}$$

In Eq. (6), for example, u_{*j} denotes the "u" component at the jth node. Similarly, $\{q_1\}$ is a vector composed of many σ_N and σ_{NT} components at many discrete points, which is expressed as

$$\{q_1\} = \{\sigma_{N,*1} \;\; \sigma_{NT,*1} \;\; \cdots \sigma_{N,*j} \;\; \sigma_{NT,*j} \;\; \cdots \;\; \sigma_{N,*M} \;\; \sigma_{NT,*M}\}^T \tag{7}$$

In Eq. (7), for example, $\sigma_{N,*j}$ denotes the σ_N component at the jth node.

Similarly, the problem shown by Fig. 3(b) is devoted to an interior boundary value problem with the outer boundary Γ_2 and the elastic constants (G_2, ν_2). The applied displacement and the traction along the boundary Γ_2 are denoted by $\{u_2\}$ and $\{q_2\}$, respectively.

In addition, the problem shown by Fig. 3(c) is devoted to a problem of the triply-connected region bounded by the inner boundaries Γ_1 and Γ_2 and the outer boundary Γ_3. For the region, the elastic constants are denoted by (G_3, ν_3). From the continuous condition for the displacement and reciprocal property of traction, the same displacement $\{u_1\}$ and traction $\{q_1\}$ in Fig. 3(a) are applied on the boundary Γ_1, and the same displacement $\{u_2\}$ and traction $\{q_2\}$ in Fig. 3(b) are applied on the boundary Γ_2. In addition, the traction vector $\{q_3\}$ applied along the outer boundary Γ_3 is given beforehand.

For two interior BVPs shown by Fig. 3(a) and (b), after discretization to Eq. (1), the BIEs can be converted in the following matrix representation form

$$[H_1]\{u_1\} = [G_1]\{q_1\}, \quad (t_o \in \Gamma_1 \text{ in Fig. 3(a)}) \tag{8}$$

$$[H_2]\{u_2\} = [G_2]\{q_2\} \quad (t_o \in \Gamma_2 \text{ in Fig. 3(b)}) \tag{9}$$

where $[H_1]$ is a matrix derived from a discretization of left hand term of Eq. (1), and $[G_1]$ from the right hand term of Eq. (1). In Eq. (8), the vector $\{u_1\}$ is composed of many u and v components for discrete points along Γ_1, which has been defined previously by Eq. (6). Similarly, the vector $\{q_1\}$ is composed of many σ_N and σ_{NT} components for discrete points along Γ_1, which has been defined previously by Eq. (7). In addition, the matrices $[H_2]$, $[G_2]$ and vectors $\{u_2\}$ and $\{q_2\}$ have a similar meaning. Clearly, one should use the elastic constants G_1 and ν_1 for the formulation of the matrices $[H_1]$ and $[G_1]$, and G_2 and ν_2 for $[H_2]$ and $[G_2]$.

It is known that, it the real size does not reach the degenerate scale, the matrices $[G_1]$ and $[G_2]$ are invertible (Vodicka and Mantic, 2004, 2008). In this case, from Eqs. (8) and (9), we have

$$\{q_1\} = [A_1]\{u_1\}, \quad \text{with } [A_1] = [G_1^{-1}][H_1] \tag{10}$$

$$\{q_2\} = [A_2]\{u_2\}, \quad \text{with } [A_2] = [G_2^{-1}][H_2] \tag{11}$$

In Eqs. (10) and (11), $[G_1^{-1}]$ and $[G_2^{-1}]$ are the inverse matrix for $[G_1]$ and $[G_2]$, respectively. In Eq. (10), the matrix $[G_1^{-1}]$, or the inverse of the matrix $[G_1]$, is obtained numerically by using a subroutine in the FORTRAN program. In any personal computer, it is easy to obtain the inverse of a matrix.

For the problem of the triply-connected region shown by Fig. 3(c), after discretization for BIE shown by Eq. (5), we have

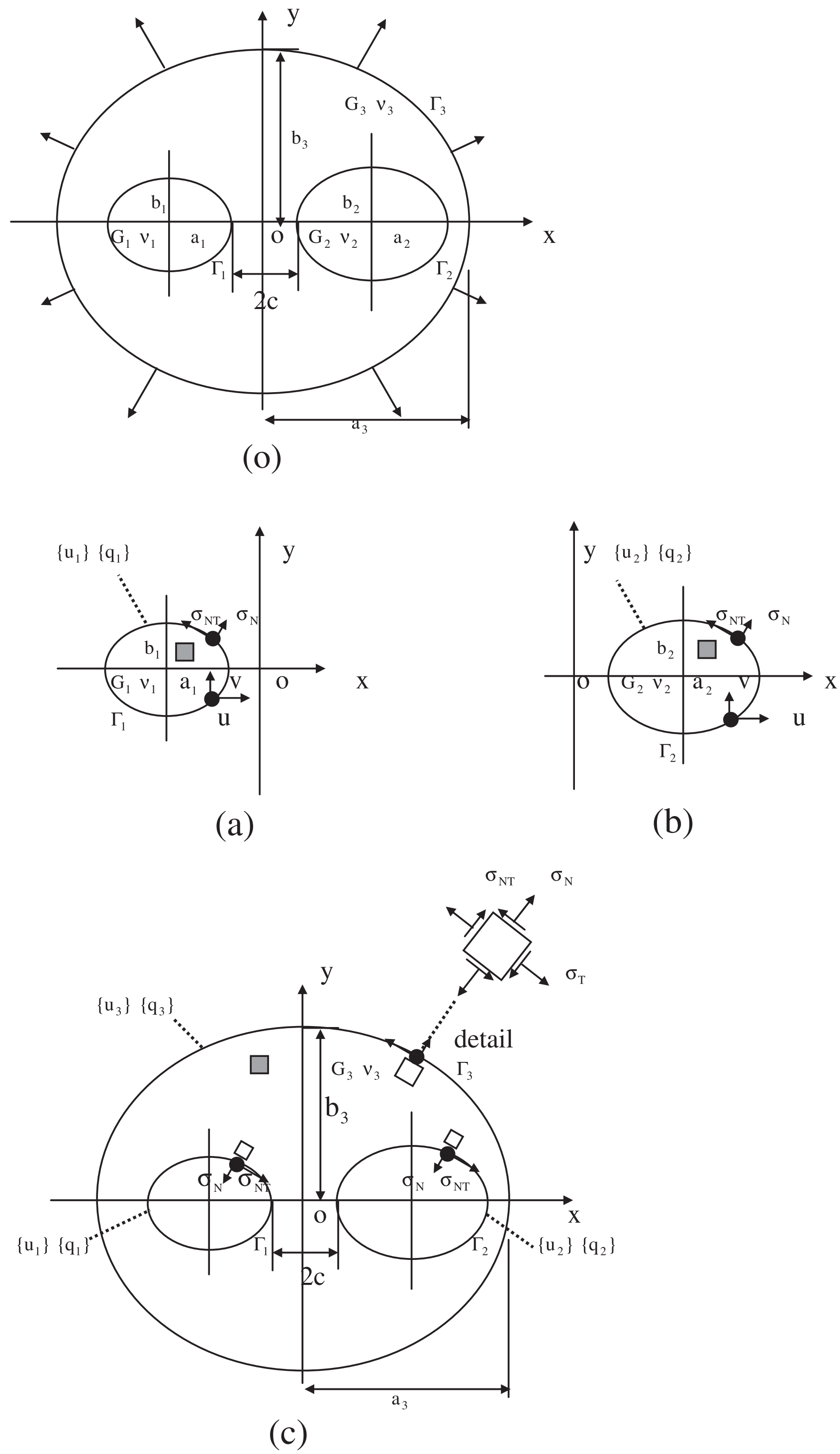

Fig. 3. Decomposition of the original problem "o" into three boundary value problems "a", "b" and "c": (o) a finite plate with elastic constants (G_3, ν_3) having two dissimilar inclusions with elastic constants (G_1, ν_1) and (G_2, ν_2), (a) a finite plate with the boundary Γ_1 and the elastic constants (G_1, ν_1), (b) a finite plate with the boundary Γ_2 and the elastic constants (G_2, ν_2), (c) a boundary value problem for a triply-connected region with elastic constants (G_3, ν_3) bounded by boundaries Γ_1 and Γ_2 and Γ_3, (▭) region defined.

$$[H_{11}]\{u_1\} + [H_{12}]\{u_2\} + [H_{13}]\{u_3\} = [G_{11}]\{q_1\} + [G_{12}]\{q_2\} + [G_{13}]\{q_3\} \quad (t_o \in \Gamma_1 \text{ in Fig. 3(c)}) \tag{12}$$

$$[H_{21}]\{u_1\} + [H_{22}]\{u_2\} + [H_{23}]\{u_3\} = [G_{21}]\{q_1\} + [G_{22}]\{q_2\} + [G_{23}]\{q_3\} \quad (t_o \in \Gamma_2 \text{ in Fig. 3(c)}) \tag{13}$$

$$[H_{31}]\{u_1\} + [H_{32}]\{u_2\} + [H_{31}]\{u_3\} = [G_{31}]\{q_1\} + [G_{32}]\{q_2\} + [G_{33}]\{q_3\} \quad (t_o \in \Gamma_3 \text{ in Fig. 3(c)}) \tag{14}$$

In Eq. (12), $[H_{11}]$, $[H_{12}]$, $[H_{13}]$ are three matrices derived from a discretization of left hand terms of Eq. (5), and $[G_{11}]$, $[G_{11}]$, $[G_{13}]$ from the right hand terms of Eq. (5). The other matrices in Eqs. (13) and (14) are derived in a similar manner.

In all matrices, the first footnote denotes where the observation point t_o is located, and the second footnote denotes where the integration point "t" and dt are located. For example, in the matrix $[H_{12}]$, t_o is located along the contour Γ_1, and the integration point "t" and "dt" are located on the boundary Γ_2.

Clearly, the matrices $[H_{11}]$ and $[G_{11}]$ are evaluated from t_o on Γ_1 and "t", "dt" on Γ_1. In this case we will meet singular kernel $1/(t-t_o)$or weaker singular kernel $\ln|t-t_o|$ in the discretization. Particularly, the matrix $[H_{11}]$ contains the term $U_1(t_o)/2$ in Eq. (5). Clearly, the matrices $[H_{22}]$, $[G_{22}]$, $[H_{33}]$ and $[G_{33}]$ have the same property.

The matrices $[H_{12}]$ and $[G_{12}]$ are evaluated from t_o on Γ_1 and "t", "dt" on Γ_2. In this case, all integrals are regular in the discretization. In addition, the matrices $[H_{jk}]$ and $[G_{jk}]$ $(j \neq k)$ possess the same property. Clearly, one should use the elastic constants G_3 and ν_3 for the formulation of all the matrices from $[H_{11}]$, $[H_{12}]$, ... to $[G_{33}]$.

Substituting Eqs. (10) and (11) into Eqs. (12)–(14) yields

$$[B_{11}]\{u_1\} + [B_{12}]\{u_2\} + [H_{13}]\{u_3\} = \{r_1\} \tag{15}$$

$$[B_{21}]\{u_1\} + [B_{22}]\{u_2\} + [H_{23}]\{u_3\} = \{r_2\} \tag{16}$$

$$[B_{31}]\{u_1\} + [B_{32}]\{u_2\} + [H_{33}]\{u_3\} = \{r_3\} \tag{17}$$

where

$$[B_{11}] = [H_{11}] - [G_{11}][A_1], \quad [B_{12}] = [H_{12}] - [G_{12}][A_2] \tag{18}$$

$$[B_{21}] = [H_{21}] - [G_{21}][A_1], \quad [B_{22}] = [H_{22}] - [G_{22}][A_2] \tag{19}$$

$$[B_{31}] = [H_{31}] - [G_{31}][A_1], \quad [B_{32}] = [H_{32}] - [G_{32}][A_2], \tag{20}$$

$$\{r_1\} = [G_{13}]\{q_3\}, \tag{21}$$

$$\{r_2\} = [G_{23}]\{q_3\} \tag{22}$$

$$\{r_3\} = [G_{33}]\{q_3\} \tag{23}$$

Note that, the vector $\{q_3\}$ is given beforehand, which is from the boundary condition along the outer boundary Γ_3.

Finally, Eqs. (15)–(17) become the governing equation for evaluating three vectors $\{u_1\}$, $\{u_2\}$ and $\{u_3\}$. The solutions for $\{u_1\}$, $\{u_2\}$ and $\{u_3\}$ can be obtained from the linear algebraic equations shown by Eqs. (15)–(17). From $\{u_1\}$ and Eq. (10), we can get the vector $\{q_1\}$. Similarly, From $\{u_2\}$ and Eq. (11), we can get the vector $\{q_2\}$.

For evaluating the hoop stress σ_T, the following technique is suggested (Chen and Wang, 2011). In fact, in the plane strain case, the strain component ε_T (in T-direction) can be expressed as (Figs. 2 and 3(c))

$$\varepsilon_T = \frac{1}{E}(\sigma_T(1-\nu^2) - \nu(1+\nu)\sigma_N) \tag{24}$$

or

$$\sigma_T = \frac{E\varepsilon_T + \nu(1+\nu)\sigma_N}{1-\nu^2}, \tag{25}$$

where E is the Young's modulus of elasticity. In Eq. (25), the component σ_N is from the vector $\{q\}$, and ε_T is the strain in the T-direction, which can be evaluated from the numerical solution of displacements along the boundary. The elongation of a boundary element can be found from the displacement solution, and the strain ε_T can be evaluated accordingly. In fact, the strain ε_T along boundary can be found in the following way. It is assume that there is an interval $\overline{AB}$ on the boundary, which is denoted by a vector $\vec{dt}$ with the length ds (Figs. 2 and 3(c)). In addition, assume that the end point "A" is fixed ($u_A = 0$, $v_A = 0$) and the end point "B" has a displacement $\Delta u + i\Delta v$, where $\Delta u = u_B - u_A = u_B$ and $\Delta v = v_B - v_A = v_B$. The projection of $\Delta u + i\Delta v$ on the direction for the vector $\vec{dt}$ is denoted by ΔL. Finally, we can evaluate ε_T by the following equation

$$\varepsilon_T = \frac{\Delta L}{ds} \tag{26}$$

Thus, the values of σ_T at many discrete points along the boundary can be evaluated.

From computed vectors $\{u_1\}$ and $\{q_1\}$ along Γ_1, we can evaluate the σ_T at both sides of Γ_1 by using Eq. (25). If one evaluates σ_T at the inclusion side, one should use the elastic constants G_1 and ν_1 for the right inclusion. On the contrary, if one evaluates σ_T at the matrix side, one should use the elastic constants G_3 and ν_3. Similarly, from the computed vectors $\{u_2\}$ and $\{q_2\}$ along Γ_2, we can evaluate the σ_T at both sides of the interface Γ_2. In addition, from $\{u_3\}$ and $\{q_3\}$ along Γ_3, we can evaluate the σ_T along the boundary Γ_3.

3. Numerical examples

Several numerical examples are provided to prove the efficiency of the suggested method. In the examples, the shear moduli G_i (i = 1, 2, 3) are subject to change, and $\nu_1 = \nu_2 = \nu_3 = 0.3$. The plane strain condition is assumed. Stress concentration factors (SCFs) along the contour and the non-dimensional stress for σ_T at both sides of interface are evaluated in all examples.

3.1. Example 1

In the first example, one elliptic inclusion with the elastic constants G_1, ν_1 is embedded in the matrix medium with the elastic constants G_2, ν_2 (Fig. 4). Simply deleting some terms in the formulation for the case of two inclusions, the derivation introduced in second section can be used to the present case accordingly.

The plate is applied by the loading $\sigma_N = p$, $\sigma_{NT} = 0$ along the outer boundary Γ_2. The elliptic interface boundary Γ_1 has two half-axis a_1,b_1, and the ellipse Γ_2 has two half-axis a_2,b_2. We assume $b_1/a_1 = b_2/a_2$ in the example. In computation, $M = 96$ divisions are used for the discretization for the contour Γ_2, and $M = 48$ (or 72) divisions are used for the discretization for the interface boundary Γ_1

In the example, for the following cases: (a) $G_1/G_2 = 10^{-5}$, 0.1, 0.5,1, 2 and 10, (b) $b_1/a_1 = b_2/a_2 = 0.25$, 0.5.0.75 and 1.0, (c) $a_1/a_2 = 0.1, 0.2, \ldots, 0.6$, the non-dimensional stress component σ_T at the points D, E and F are expressed as (Fig. 4)

$$\sigma_{T,D} = s_D(G_1/G_2, b_2/a_2, a_1/a_2)p, \quad \sigma_{T,E} = s_E(G_1/G_2, b_2/a_2, a_1/a_2)p,$$
$$\sigma_{T,F} = s_F(G_1/G_2, b_2/a_2, a_1/a_2)p \tag{27}$$

The computed non-dimensional stresses for σ_T, or $s_D(G_1/G_2, b_2/a_2, a_1/a_2)$, $s_E(G_1/G_2, b_2/a_2, a_1/a_2)$ and $s_F(G_1/G_2, b_2/a_2, a_1/a_2)$ are listed in Table 1.

From the tabulated results we see following results. In the case of $G_1/G_2 = 10^{-5}$, 0.1, 0.2, or 0.5, or in the softer inclusion case, gen-

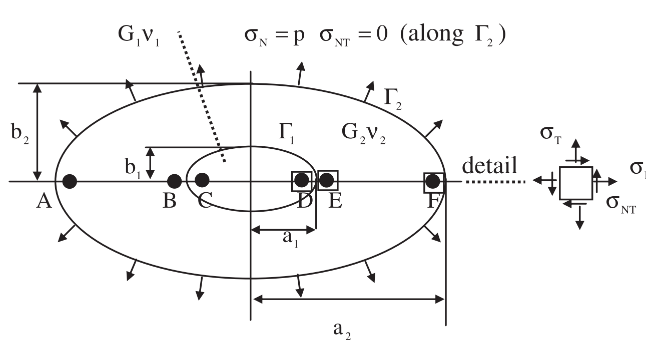

Fig. 4. A finite elliptic plate with the elastic constants (G_2, ν_2) containing one dissimilar elliptic inclusion with the elastic constants $(G_1\nu_1)$.

Table 1
The non-dimensional stresses ($=\sigma_T/p$) $s_D(G_1/G_2, b_2/a_2, a_1/a_2)$, $s_E(G_1/G_2, b_2/a_2, a_1/a_2)$ and $s_F(G_1/G_2, b_2/a_2, a_1/a_2)$ at the point "D" (in inclusion) and "E" and "F" (in matrix), under different G_1/G_2 ratios (see Fig. 4 and Eq. (27)).

b_2/a_2	a_1/a_2					
	0.1	0.2	0.3	0.4	0.5	0.6
(1a) S_D values in $G_1/G_2 = 10^{-5}$ case						
0.25	0.0001	0.0002	0.0002	0.0003	0.0005	0.0007
0.50	0.0001	0.0001	0.0001	0.0001	0.0001	0.0002
0.75	0.0000	0.0000	0.0000	0.0001	0.0001	0.0001
1.00	0.0000	0.0000	0.0000	0.0000	0.0000	0.0001
(1b) S_E values in $G_1/G_2 = 10^{-5}$ case						
0.25	9.6284	13.3771	18.6930	25.4187	34.4539	46.7233
0.50	4.2920	4.9901	6.1622	7.8780	10.5604	14.9508
0.75	2.7750	3.0074	3.4323	4.1098	5.2547	7.2523
1.00	2.0455	2.1102	2.2277	2.4035	2.6946	3.1628
1.00[a]	2.0202	2.0833	2.1978	2.3810	2.6667	3.1250
(1c) S_F values in $G_1/G_2 = 10^{-5}$ case						
0.25	0.9830	0.9832	0.9843	0.9875	0.9879	0.9200
0.50	0.9883	0.9643	0.8959	0.7156	0.2482	−0.9634
0.75	0.9948	0.9850	0.9514	0.8560	0.6098	−0.0009
1.00	1.0181	1.0819	1.1978	1.3812	1.6696	2.1333
1.00[a]	1.0202	1.0833	1.1978	1.3810	1.6667	2.1250
(2a) S_D values in $G_1/G_2 = 0.1$ case						
0.25	0.5639	0.6167	0.6363	0.6242	0.6078	0.5951
0.50	0.3895	0.4175	0.4553	0.4906	0.5186	0.5324
0.75	0.3188	0.3315	0.3523	0.3788	0.4117	0.4455
1.00	0.2854	0.2918	0.3031	0.3190	0.3443	0.3813
(2b) S_E values in $G_1/G_2 = 0.1$ case						
0.25	4.4052	4.8041	4.8750	4.7166	4.5172	4.3668
0.50	2.8706	3.1143	3.4241	3.6927	3.8613	3.8960
0.75	2.1530	2.2626	2.4412	2.6709	2.9411	3.1973
1.00	1.7467	1.7857	1.8549	1.9554	2.1105	2.3372
(2c) S_F values in $G_1/G_2 = 0.1$ case						
0.25	0.9830	0.9830	0.9832	0.9834	0.9829	0.9779
0.50	0.9911	0.9797	0.9533	0.9030	0.8235	0.7260
0.75	0.9967	0.9956	0.9896	0.9753	0.9582	0.9764
1.00	1.0122	1.0573	1.1370	1.2587	1.4379	1.6997
(3a) S_D values in $G_1/G_2 = 0.5$ case						
0.25	0.8953	0.9033	0.9016	0.9055	0.8998	0.8945
0.50	0.8454	0.8561	0.8673	0.8757	0.8784	0.8781
0.75	0.8073	0.8148	0.8258	0.8379	0.8501	0.8616
1.00	0.7819	0.7871	0.7960	0.8079	0.8249	0.8467
(3b) S_E values in $G_1/G_2 = 0.5$ case						
0.25	1.4733	1.4847	1.4763	1.4841	1.4687	1.4539
0.50	1.3715	1.3907	1.4089	1.4221	1.4211	1.4137
0.75	1.2868	1.3001	1.3189	1.3400	1.3583	1.3731
1.00	1.2267	1.2349	1.2488	1.2684	1.2951	1.3293
(3c) S_F values in $G_1/G_2 = 0.5$ case						
0.25	0.9829	0.9830	0.9830	0.9830	0.9828	0.9820
0.50	0.9937	0.9923	0.9898	0.9866	0.9839	0.9849
0.75	0.9975	1.0002	1.0053	1.0147	1.0314	1.0611
1.00	1.0021	1.0154	1.0381	1.0709	1.1144	1.1702
(4a) S_D values in $G_1/G_2 = 1$ case						
0.25	0.9721	0.9720	0.9721	0.9872	0.9873	0.9874
0.50	0.9932	0.9931	0.9930	0.9969	0.9969	0.9969
0.75	0.9976	0.9975	0.9974	0.9987	0.9986	0.9986
1.00	0.9992	0.9991	0.9990	0.9994	0.9993	0.9992
(4b) S_E values in $G_1/G_2 = 1$ case						
0.25	0.9721	0.9720	0.9721	0.9872	0.9873	0.9874
0.50	0.9932	0.9931	0.9930	0.9969	0.9969	0.9969
0.75	0.9976	0.9975	0.9974	0.9987	0.9986	0.9986
1.00	0.9992	0.9991	0.9990	0.9994	0.9993	0.9992
(4c) S_F values in $G_1/G_2 = 1$ case						
0.25	0.9829	0.9829	0.9829	0.9829	0.9829	0.9830
0.50	0.9942	0.9942	0.9942	0.9942	0.9943	0.9943
0.75	0.9967	0.9967	0.9966	0.9966	0.9965	0.9964
1.00	0.9976	0.9975	0.9973	0.9973	0.9971	0.9968
(5a) S_D values in $G_1/G_2 = 2$ case						
0.25	1.0265	1.0206	1.0195	1.0398	1.0444	1.0495
0.50	1.0912	1.0842	1.0770	1.0786	1.0780	1.0804
0.75	1.1303	1.1239	1.1151	1.1085	1.0995	1.0915
1.00	1.1604	1.1546	1.1451	1.1338	1.1174	1.0980
(5b) S_E values in $G_1/G_2 = 2$ case						
0.25	0.8002	0.7933	0.7875	0.7912	0.7884	0.7862
0.50	0.8129	0.8076	0.8011	0.7978	0.7932	0.7900
0.75	0.8219	0.8175	0.8110	0.8046	0.7965	0.7882
1.00	0.8304	0.8262	0.8194	0.8107	0.7990	0.7851
(5c) S_F values in $G_1/G_2 = 2$ case						
0.25	0.9829	0.9829	0.9829	0.9830	0.9831	0.9835
0.50	0.9942	0.9944	0.9943	0.9935	0.9913	0.9857
0.75	0.9955	0.9917	0.9849	0.9744	0.9593	0.9379
1.00	0.9943	0.9844	0.9680	0.9457	0.9176	0.8844
(6a) S_D values in $G_1/G_2 = 10$ case						
0.25	1.1053	1.0869	1.0761	1.0934	1.1022	1.1133
0.50	1.1900	1.1768	1.1615	1.1598	1.1602	1.1691
0.75	1.2643	1.2515	1.2334	1.2187	1.2012	1.1873
1.00	1.3324	1.3188	1.2967	1.2704	1.2341	1.1924
(6b) S_E values in $G_1/G_2 = 10$ case						
0.25	0.8667	0.8333	0.7921	0.7545	0.7213	0.6934
0.50	0.7265	0.7148	0.6977	0.6785	0.6579	0.6383
0.75	0.6751	0.6677	0.6561	0.6417	0.6245	0.6058
1.00	0.6503	0.6436	0.6329	0.6187	0.6010	0.5807
(6c) S_F values in $G_1/G_2 = 10$ case						
0.25	0.9829	0.9829	0.9830	0.9831	0.9834	0.9841
0.50	0.9940	0.9932	0.9913	0.9874	0.9800	0.9659
0.75	0.9935	0.9839	0.9676	0.9440	0.9124	0.8706
1.00	0.9908	0.9705	0.9376	0.8932	0.8391	0.7770

[a] From an exact solution for the thick-walled cylinder.

erally, $s_D < s_E$. In this case, the point "E" is under more dangerous situation.

In the case of $G_1/G_2 = 10^{-5}$, the s_D values are nearly equal to zero. Since a very soft inclusion, or $G_1 \approx 0$, has no ability to resist the deformation, this phenomenon is easy to understand. In this case, the interface portion at the matrix side is nearly under traction free condition, and the non-dimensional stress concentration factor, or the value σ_T/p can reach a huge value. For example, we have $s_E = 46.7233$ in the case of $G_1/G_2 = 10^{-5}$, $b_2/a_2 = 0.25$ and $a_1/a_2 = 0.6$.

It is known that for an elliptic notch with two half-axis a_1, b_1 and the remote tension $\sigma_x^\infty = \sigma_y^\infty = p$, we have $s_E = 8$, 4, 2.667 and 2 for $b_1/a_1 = 0.25$, 0.5 0.75 and 1, respectively. In addition, in the case of $a_1/a_2 = 0.1$, we have $s_E = 9.2684$, 4.2920, 2.7750 and 2.0455, respectively. Clearly, two sets of the results are comparable.

Secondly, when $b_1/a_1 = b_2/a_2 = 1$ and $G_1/G_2 = 10^{-5}$, the studied problem will approximate a problem for a thick-walled cylinder with $\sigma_N = p$ applied along the outer boundary Γ_2. From the solution for the thick cylinder, we have $s_E = 2.0202$, 2.0833, 2.1978, 2.3810, 2.6667, 3.1250 for $a_1/a_2 = 0.1$, 0.2, 0.3, 0.4, 0.5 and 0.6, respectively. In the meantime, the relevant values are $s_E = 2.0455$, 2.1102, 2.2277, 2.4035, 2.6946 and 3.1628, respectively. Two sets of results coincide closely. This can partly prove that accurate results have been achieved in the paper.

In the case of $G_1/G_2 = 1$, the problem becomes a perfect plate under the tension $\sigma_N = p$ along the outer boundary Γ_2. In this case, the exact solution is $s_D = s_E = s_F = 1$. However, the relevant computed values are changing from 0.9932 to 0.9968, for the case of $b_2/a_2 \geqslant 0.5$. That is to say a higher accuracy has been achieved in the present method.

In the case of $G_1/G_2 = 2$ and 10, or in the more rigid inclusion case, generally, we find $s_D > s_E$. $s_D > s_F$. In this case, the point "D" is under a higher level of stress. From tabulated results we see that

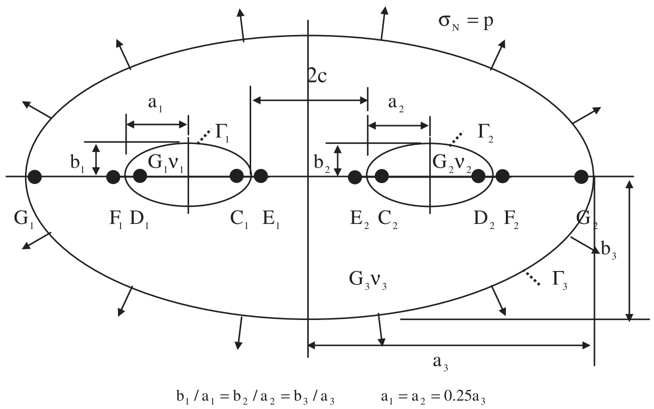

Fig. 5. A finite elliptic plate with the elastic constants (G_3, ν_3) containing two dissimilar elliptic inclusions with the elastic constants ($G_1\nu_1$) and (G_2, ν_2).

we have $s_D > 1$, $s_E < 1$, $s_F < 1$ in general. In the case of G_1/G_2=10, the s_D values vary within the range of 1.1053–1.3324, the s_E values vary within the range of 0.8667–0.5807, the s_F values vary within the range of 0.9940–0.7770. That is to say a more rigid inclusion does not cause a serious situation for the stress distribution.

3.2. Example 2

In the second example, two elliptic inclusions with the elastic constants G_1, ν_1, G_2, ν_2 are embedded in the matrix medium with the elastic constants G_3, ν_3 (Fig. 5). Therefore, the derivation introduced in second section can be used to the present case directly.

The plate is applied by the loading $\sigma_N = p$, $\sigma_{NT} = 0$ along the outer boundary Γ_3. The elliptic interface boundaries Γ_1, Γ_2 have two half-axes a_1, b_1, and a_2, b_2, respectively. For two inclusions, we assume $a_1 = a_2$ and $b_1 = b_2$. The ellipse Γ_3 has two half-axes a_3, b_3, and we assume $b_1/a_1 = b_2/a_2 = b_3/a_3$ and choose $a_1 = a_2 = 0.25a_3$ in the example. The spacing between two inclusions is denoted by "2c". In computation, $M = 96$ divisions are used for the discretization of the contour Γ_3, and $M = 48$ divisions are used for the discretization for the interface boundaries Γ_1 and Γ_2.

In the example, for the following cases: (a) $G_1/G_3 = G_2/G_3 = 10^{-5}$, 0.1, and 10, (b) $b_1/a_1 = b_2/a_2 = b_3/a_3 = 0.5$ and 1.0, (c) $c/a_3 = 0.05$, 0.1, 0.15, ..., 0.4, the non-dimensional stress component σ_T at the points C_1, D_1, E_1, F_1, G_1 are expressed as (Fig. 5)

$$\begin{aligned}
&\sigma_{T,C} = s_C(G_1/G_3, b_3/a_3, c/a_3)p, \quad \sigma_{T,D} = s_D(G_1/G_3, b_3/a_3, c/a_3)p,\\
&\sigma_{T,E} = s_E(G_1/G_3, b_3/a_3, c/a_3)p, \quad \sigma_{T,F} = s_F(G_1/G_3, b_3/a_3, c/a_3)p,\\
&\sigma_{T,G} = s_G(G_1/G_3, b_3/a_3, c/a_3)p
\end{aligned} \tag{28}$$

Clearly, at the points C_2, D_2, E_2, F_2, G_2, the relevant values are the same.

The computed non-dimensional stresses for σ_T, or $s_C(G_1/G_3, b_3/a_3, c/a_3)$, $s_D(G_1/G_3, b_3/a_3, c/a_3)$, $s_E(G_1/G_3, b_3/a_3, c/a_3)$, $s_F(G_1/G_3, b_3/a_3, c/a_3)$ and $s_G(G_1/G_3, b_3/a_3, c/a_3)$ are listed in Table 2.

From the tabulated results we see following results. In the case of G_1/G_3=10^{-5}, the s_C and s_D values are equal to zero. Since a very soft inclusion, or $G_1 \approx 0$, has no ability to resist the deformation, this phenomenon is easy to understand. In addition, in the case of b_3/a_3=0.5 and c/a_3=0.05, for two points $E_1$and F_1 embedded in the matrix medium, we have $s_E = 8.817$, $s_F = 6.266$ ($s_E > s_F$), respectively. This is indeed the phenomenon of the stress concentration. However, in the case of b_3/a_3=0.5 and c/a_3=0.4 we have $s_E = 6.008$, $s_F = 9.079$ ($s_E < s_F$), respectively. That is to say when c/a_3 changes from 0.05 to 0.4, the stress distribution in the matrix medium will be changed significantly.

In the case of G_1/G_3=0.1, the inclusion is softer than the matrix medium. In this case, we have $s_C < s_E$ and $s_D < s_F$ in general. For example, in the case of b_3/a_3=0.5 and c/a_3=0.05, we have s_C=0.557 and s_E=4.560. Note that, for example, s_C, s_E denote the non-dimensional stress at two sides of interface boundary. Since a softer medium has a lower stress for the same amount of deformation (or stress = $G *$ stain), this phenomenon is easy to realize. In addition, the role of the softer inclusion is significant. For example, in the case of $b_3/a_3 = 0.5$ and $c/a_3 = 0.05$, we have $s_E = 8.817$ (for $G_1/G_3 = 10^{-5}$) and $s_E = 4.560$ (for $G_1/G_3 = 0.1$), respectively. That is to say even a rather softer inclusion is adhered to the matrix medium, the stress concentration factor will be lowered significantly.

In the case of $G_1/G_3 = 10$, the inclusion is more rigid than the matrix medium. In this case, we have $s_C > s_E$ and $s_D > s_F$ in general. For example, in the case of $b_3/a_3 = 0.5$ and $c/a_3 = 0.05$, we have $s_C = 1.063$ and $s_E = 0.831$. However, in the studied ranges for b_3/a_3 and c/a_3, all values for s_C, s_D, s_E, s_F and s_G change within the range from 0.507 to 1.350. That is to say a more rigid inclusion does

Table 2
The non-dimensional stresses (=σ_T/p), $s_C(G_1/G_3, b_3/a_3, c/a_3)$, $s_D(G_1/G_3, b_3/a_3, c/a_3)$, $s_E(G_1/G_3, b_3/a_3, c/a_3)$, $s_F(G_1/G_3, b_3/a_3, c/a_3)$, $s_G(G_1/G_3, b_3/a_3, c/a_3)$at the points C_i,D_i (in inclusion, i = 1, 2) and E_i, F_i G_i, (in matrix, i = 1, 2), under different $G_1/G_3 = G_2/G_3$ ratios (see Fig. 5 and Eq. (28)).

b_3/a_3	c/a_3							
	0.05	0.10	0.15	0.20	0.25	0.30	0.35	0.40
(1a) S_c values in $G_1/G_3 = G_2/G_3 = 10^{-5}$ case								
0.5	0.000	0.000	0.000	0.000	0.000	0.000	0.000	0.000
1.0	0.000	0.000	0.000	0.000	0.000	0.000	0.000	0.000
(1b) S_D values in $G_1/G_3 = G_2/G_3 = 10^{-5}$ case								
0.5	0.000	0.000	0.000	0.000	0.000	0.000	0.000	0.000
1.0	0.000	0.000	0.000	0.000	0.000	0.000	0.000	0.000
(1c) S_E values in $G_1/G_3 = G_2/G_3 = 10^{-5}$ case								
0.5	8.817	6.581	5.787	5.464	5.390	5.477	5.683	6.008
1.0	4.859	3.593	3.070	2.762	2.556	2.412	2.311	2.245
(1d) S_F values in $G_1/G_3 = G_2/G_3 = 10^{-5}$ case								
0.5	6.266	5.929	5.934	6.112	6.433	6.924	7.694	9.079
1.0	2.984	2.735	2.619	2.568	2.570	2.632	2.801	3.242
(1e) S_G values in $G_1/G_3 = G_2/G_3 = 10^{-5}$ case								
0.5	0.773	0.777	0.757	0.721	0.673	0.616	0.569	0.632
1.0	1.303	1.446	1.603	1.801	2.073	2.475	3.130	4.354
(2a) S_c values in $G_1/G_3 = G_2/G_3 = 0.1$ case								
0.5	0.577	0.493	0.460	0.444	0.438	0.438	0.441	0.447
1.0	0.429	0.370	0.346	0.333	0.326	0.322	0.323	0.329
(2b) S_D values in $G_1/G_3 = G_2/G_3 = 0.1$ case								
0.5	0.460	0.451	0.451	0.456	0.465	0.478	0.498	0.531
1.0	0.340	0.331	0.329	0.331	0.337	0.349	0.374	0.427
(2c) S_E values in $G_1/G_3 = G_2/G_3 = 0.1$ case								
0.5	4.560	3.747	3.417	3.260	3.193	3.179	3.193	3.218
1.0	3.268	2.615	2.324	2.150	2.032	1.950	1.891	1.853
(2d) S_F values in $G_1/G_3 = G_2/G_3 = 0.1$ case								
0.5	3.449	3.396	3.414	3.473	3.568	3.703	3.902	4.236
1.0	2.215	2.116	2.069	2.054	2.070	2.128	2.262	2.591
(2e) S_G values in $G_1/G_3 = G_2/G_3 = 0.1$ case								
0.5	0.912	0.913	0.911	0.910	0.915	0.935	1.001	1.203
1.0	1.239	1.325	1.423	1.547	1.715	1.955	2.325	2.951
(3a) S_c values in $G_1/G_3 = G_2/G_3 = 10$ case								
0.5	1.063	1.104	1.132	1.151	1.164	1.175	1.183	1.191
1.0	1.161	1.187	1.227	1.258	1.284	1.306	1.327	1.350
(3b) S_D values in $G_1/G_3 = G_2/G_3 = 10$ case								
0.5	1.138	1.140	1.137	1.130	1.117	1.095	1.058	0.984
1.0	1.216	1.224	1.220	1.205	1.177	1.131	1.056	0.928
(3c) S_E values in $G_1/G_3 = G_2/G_3 = 10$ case								
0.5	0.831	0.749	0.722	0.710	0.702	0.697	0.693	0.688
1.0	0.766	0.683	0.654	0.641	0.632	0.627	0.622	0.618
(3d) S_F values in $G_1/G_3 = G_2/G_3 = 10$ case								
0.5	0.706	0.699	0.693	0.687	0.678	0.665	0.645	0.611
1.0	0.626	0.620	0.613	0.605	0.593	0.577	0.555	0.521
(3e) S_G values in $G_1/G_3 = G_2/G_3 = 10$ case								
0.5	0.967	0.958	0.944	0.923	0.891	0.845	0.773	0.659
1.0	0.846	0.832	0.809	0.777	0.733	0.676	0.601	0.507

Table 3
The non-dimensional stresses (=σ_T/p), $s_{C1}(G_1/G_3, G_2/G_3, b_3/a_3, c/a_3)$, $s_{D1}(G_1/G_3, G_2/G_3, b_3/a_3, c/a_3)$, $s_{E1}(G_1/G_3, G_2/G_3, b_3/a_3, c/a_3)$, $s_{F1}(G_1/G_3, G_2/G_3, b_3/a_3, c/a_3)$, $s_{G1}(G_1/G_3, G_2/G_3, b_3/a_3, c/a_3)$, $s_{C2}(G_1/G_3, G_2/G_3, b_3/a_3, c/a_3)$, $s_{D2}(G_1/G_3, G_2/G_3, b_3/a_3, c/a_3)$, $s_{E2}(G_1/G_3, G_2/G_3, b_3/a_3, c/a_3)$, $s_{F2}(G_1/G_3, G_2/G_3, b_3/a_3, c/a_3)$, $s_{G2}(G_1/G_3, G_2/G_3, b_3/a_3, c/a_3)$, at the points C_i, D_i (in inclusion, i = 1, 2) and E_i, F_i G_i, (in matrix, i = 1, 2), under conditions (a) $G_1/G_3 = 10^{-5}$ $G_2/G_3 = 10^5$, (b) $G_1/G_3 = 0.1$ $G_2/G_3 = 10$ (see Fig. 5, Eqs. (29) and (30)).

b_3/a_3	c/a_3							
	0.05	0.10	0.15	0.20	0.25	0.30	0.35	0.40
(1a) S_{C1} values in the case of $G_1/G_3 = 10^{-5}$ and $G_2/G_3 = 10^5$								
0.5	0.000	0.000	0.000	0.000	0.000	0.000	0.000	0.000
1.0	0.000	0.000	0.000	0.000	0.000	0.000	0.000	0.000
(1b) S_{D1} values in the case of $G_1/G_3 = 10^{-5}$ and $G_2/G_3 = 10^5$								
0.5	0.000	0.000	0.000	0.000	0.000	0.000	0.000	0.000
1.0	0.000	0.000	0.000	0.000	0.000	0.000	0.000	0.000
(1c) S_{E1} values in the case of $G_1/G_3 = 10^{-5}$ and$G_2/G_3 = 10^5$								
0.5	4.487	5.017	5.307	5.518	5.704	5.892	6.109	6.396
1.0	1.500	1.740	1.871	1.971	2.049	2.113	2.170	2.230
(1d) S_{F1} values in the case of $G_1/G_3 = 10^{-5}$ and $G_2/G_3 = 10^5$								
0.5	5.608	5.836	6.070	6.344	6.692	7.174	7.916	9.268
1.0	2.024	2.136	2.230	2.325	2.437	2.591	2.840	3.365
(1e) S_{G1} values in the case of $G_1/G_3 = 10^{-5}$ and $G_2/G_3 = 10^5$								
0.5	0.838	0.798	0.752	0.699	0.639	0.574	0.524	0.586
1.0	1.469	1.559	1.684	1.860	2.114	2.502	3.145	4.364
(1f) S_{C2} values in the case of $G_1/G_3 = 10^{-5}$ and $G_2/G_3 = 10^5$								
0.5	2.459	1.806	1.504	1.333	1.235	1.185	1.164	1.161
1.0	2.009	1.859	1.741	1.657	1.598	1.555	1.527	1.510
(1g) S_{D2} values in the case of $G_1/G_3 = 10^{-5}$ and $G_2/G_3 = 10^5$								
0.5	1.106	1.100	1.100	1.103	1.093	1.077	1.035	0.950
1.0	1.448	1.380	1.315	1.250	1.177	1.089	0.969	0.793
(1h) S_{E2} values in the case of $G_1/G_3 = 10^{-5}$ and $G_2/G_3 = 10^5$								
0.5	0.828	0.867	0.854	0.830	0.801	0.772	0.743	0.718
1.0	0.241	0.386	0.472	0.519	0.547	0.563	0.571	0.575
(1i) S_{F2} values in the case of $G_1/G_3 = 10^{-5}$ and $G_2/G_3 = 10^5$								
0.5	0.730	0.723	0.710	0.695	0.677	0.657	0.629	0.589
1.0	0.554	0.557	0.555	0.549	0.539	0.524	0.503	0.475
(1j) S_{G2} values in the case of $G_1/G_3 = 10^{-5}$ and $G_2/G_3 = 10^5$								
0.5	0.946	0.930	0.910	0.885	0.849	0.796	0.716	0.591
1.0	0.927	0.875	0.820	0.760	0.693	0.616	0.526	0.429
(2a) S_{C1} values in the case of $G_1/G_3 = 0.1$ and$G_2/G_3 = 10$								
0.5	0.388	0.412	0.424	0.432	0.438	0.444	0.449	0.455
1.0	0.246	0.270	0.282	0.290	0.298	0.305	0.315	0.327
(2b) S_{D1} values in the case of $G_1/G_3 = 0.1$ and $G_2/G_3 = 10$								
0.5	0.437	0.445	0.452	0.461	0.471	0.483	0.502	0.533
1.0	0.292	0.301	0.309	0.318	0.330	0.348	0.376	0.432
(2c) S_{E1} values in the case of $G_1/G_3 = 0.1$ and$G_2/G_3 = 10$								
0.5	2.682	2.953	3.088	3.170	3.225	3.265	3.294	3.311
1.0	1.290	1.491	1.598	1.673	1.729	1.773	1.811	1.851
(2d) S_{F1} values in the case of $G_1/G_3 = 0.1$ and $G_2/G_3 = 10$								
0.5	3.296	3.370	3.444	3.526	3.623	3.752	3.940	4.262
1.0	1.738	1.806	1.867	1.931	2.008	2.116	2.295	2.664
(2e) S_{G1} values in the case of $G_1/G_3 = 0.1$ and$G_2/G_3 = 10$								
0.5	0.935	0.924	0.914	0.907	0.908	0.927	0.992	1.195
1.0	1.322	1.382	1.465	1.580	1.740	1.976	2.343	2.975
(2f) S_{C2} values in the case of $G_1/G_3 = 0.1$ and $G_2/G_3 = 10$								
0.5	1.786	1.472	1.327	1.245	1.200	1.177	1.169	1.171
1.0	1.761	1.652	1.566	1.507	1.465	1.435	1.415	1.403
(2g) S_{D2} values in the case of $G_1/G_3 = 0.1$ and$G_2/G_3 = 10$								
0.5	1.128	1.121	1.116	1.113	1.102	1.085	1.050	0.980
1.0	1.366	1.318	1.273	1.226	1.172	1.105	1.012	0.869
(2h) S_{E2} values in the case of $G_1/G_3 = 0.1$ and$G_2/G_3 = 10$								
0.5	0.761	0.775	0.766	0.753	0.739	0.725	0.713	0.701
1.0	0.465	0.553	0.597	0.619	0.630	0.636	0.637	0.637
(2i) S_{F2} values in the case of $G_1/G_3 = 0.1$ and$G_2/G_3 = 10$								
0.5	0.709	0.706	0.700	0.691	0.681	0.667	0.646	0.611
1.0	0.623	0.620	0.614	0.605	0.593	0.575	0.550	0.514
(2j) S_{G2} values in the case of $G_1/G_3 = 0.1$ and $G_2/G_3 = 10$								
0.5	0.964	0.952	0.936	0.915	0.884	0.838	0.767	0.655
1.0	0.921	0.879	0.835	0.785	0.727	0.659	0.577	0.482

not cause a serious situation for the stress distribution in the composite medium.

3.3. Example 3

In the third example, all notations in second example are used. However, two ratios G_1/G_3 and G_2/G_3 may not be same. In the example, for the following cases: (a) $G_1/G_3 = 10^{-5}$, $G_2/G_3 = 10^5$ and $G_1/G_3 = 0.1$, $G_2/G_3 = 10$, (b) $b_1/a_1 = b_2/a_2 = b_3/a_3 = 0.5$ and 1.0, (c) $c/a_3 = 0.05, 0.1, 0.15, \ldots, 0.4$, the non-dimensional stress component σ_T at the points C_i, D_i (in inclusion, $i = 1,2$) and E_i, F_i G_i (in matrix, $i = 1,2$), are expressed as (Fig. 5)

$$\begin{aligned}
&\sigma_{T,C1} = s_{C1}(G_1/G_3, G_2/G_3, b_3/a_3, c/a_3)p,\ \sigma_{T,D1} = s_{D1}(G_1/G_3, G_2/G_3, b_3/a_3, c/a_3)p \\
&\sigma_{T,E1} = s_{E1}(G_1/G_3, G_2/G_3, b_3/a_3, c/a_3)p,\ \sigma_{T,F1} = s_{F1}(G_1/G_3, G_2/G_3, b_3/a_3, c/a_3)p \\
&\sigma_{T,G1} = s_{G1}(G_1/G_3, G_2/G_3, b_3/a_3, c/a_3)p
\end{aligned} \tag{29}$$

$$\begin{aligned}
&\sigma_{T,C2} = s_{C2}(G_1/G_3, G_2/G_3, b_3/a_3, c/a_3)p,\ \sigma_{T,D2} = s_{D2}(G_1/G_3, G_2/G_3, b_3/a_3, c/a_3)p \\
&\sigma_{T,E2} = s_{E2}(G_1/G_3, G_2/G_3, b_3/a_3, c/a_3)p,\ \sigma_{T,F2} = s_{F2}(G_1/G_3, G_2/G_3, b_3/a_3, c/a_3)p \\
&\sigma_{T,G2} = s_{G2}(G_1/G_3, G_2/G_3, b_3/a_3, c/a_3)p
\end{aligned} \tag{30}$$

The computed non-dimensional stresses for σ_T, or $s_{C1}(G_1/G_3, G_2/G_3, b_3/a_3, c/a_3), \ldots$ to $s_{G2}(G_1/G_3, G_2/G_3, b_3/a_3, c/a_3)$ are listed in Table 3.

From the tabulated results we see following results. In the case of $G_1/G_3 = 10^{-5}$ and $G_2/G_3 = 10^5$, the left interface Γ_1 is nearly under the traction free condition and the right inclusion is a very rigid one. As in the second example, the s_{C1} and s_{D1} values are equal to zero. In addition, in the case of $b_3/a_3 = 0.5$ and $c/a_3 = 0.4$, for two points $E_1$and F_1 embedded in the matrix medium, we have $s_{E1} = 6.396$, $s_{F1} = 9.268$, respectively. This is indeed the phenomenon of the stress concentration. At the right portion, in the case of $b_3/a_3 = 0.5$ and $c/a_3 = 0.05$, we have $s_{C2} = 2.459$, $s_{E2} = 0.828$ ($s_{C2} > s_{E2}$), $s_{D2} = 1.106$, $s_{F2} = 0.730$ ($s_{D2} > s_{F2}$). Since the stress σ_T in the softer side to interface must have a lower value, this phenomenon, or $s_{C2} > s_{E2}$ and $s_{D2} > s_{F2}$ is easy to understand.

The second set of computation is under the condition of $G_1/G_3 = 0.1$ and $G_2/G_3 = 10$. In the case of $b_3/a_3 = 0.5$ and $c/a_3 = 0.4$, for two points $E_1$and F_1 embedded in the matrix medium, we have $s_{E1} = 3.311$, $s_{F1} = 4.262$, respectively. Comparing with previous case (or for case $G_1/G_3 = 10^{-5}$and $G_2/G_3 = 10^5$), the s_{E1} and s_{F1} values are considerably reduced. In addition, in the studied ranges for b_3/a_3 and c/a_3, all values for s_{C2}, s_{D2}, s_{E2}, s_{F2} and s_{G2} change within the range from 0.482 to 1.786. That is to say a more rigid inclusion does not cause a serious variation for the stress distribution in the composite medium.

4. Conclusions

This paper provides a universal way to solve the dissimilar inclusion problem in a finite plate. There is no limitation for the configurations of inclusions and the surrounding plate. Because of limitation of space, only problems for the elliptic inclusions are carried out in the present paper.

The mentioned problem is decomposed into two forms of BVP. One is for an interior region, and other is for a triply-connected region. The CVBIE is suggested for two forms of BVP. The CVBIE in plane elasticity has some particular advantages. In the CVBIE, it is easy to distinguish the singular kernel from their expression. In addition, the suggested CVBIE belongs to a direct formulation of BIE. Once the displacements are evaluated from the solution of BIE, the hoop stress, or the component σ_T, is easier to evaluate, which is shown by Eqs. (24)–(26).

If one normally formulates the BIEs in matrix representation form for the case of two inclusions, the vectors $\{u_1\}$, $\{q_1\}$, $\{u_2\}$, $\{q_2\}$ (assumed on the interface boundaries Γ_1 and Γ_2) and $\{u_3\}$ (assumed on the outer boundary Γ_3) are five unknown vectors. It is a complicated work to assemble the relevant matrices into the appropriate places. To overcome this difficulty, the inverse matrix technique is suggested in the present study. In the technique, the vectors $\{q_1\}$ and $\{q_2\}$ are expressed by the vectors $\{u_1\}$ and $\{u_2\}$, respectively. After taking this step, only the three vectors $\{u_1\}$, $\{u_2\}$ and $\{u_3\}$ become unknowns, and the relevant governing algebraic equations are expressed by Eqs. (12) and (14). Therefore, we can considerably reduce the effort in the FORTRAN program.

Many possible examinations are carried out in the present study. For example, in the case of $G_1/G_2 = 1$ in the first example, all σ_T components should take the unit value (or=1). From Table 1 we see that, the computed results are $\sigma_T \approx 1$ (from 0.9932 to 0.9968 for $b_2/a_2 \geqslant 0.5$). This can partly prove that accurate results have been achieved in the present study.

References

Brebbia, C.A., Tells, J.C.F., Wrobel, L.C., 1984. Boundary Element Techniques – Theory and Application in Engineering. Springer, Heidelberg.
Chang, C.S., Conway, H.D., 1969. Stress analysis of an infinite plate containing an elastic rectangular inclusion. Acta Mech. 8, 160–173.
Chen, J.T., Chen, Y.W., 2000. Dual boundary element analysis using complex variables for potential problems with or without a degenerate boundary. Eng. Anal. Bound. Elem. 24, 671–684.
Chen, J.T., Li, Y.T., 2009. Torsional rigidity of a circular bar with multiple circular inclusions using the null-field integral approach. Comput. Mech. 44, 221–232.
Chen, Y.Z., Lin, X.Y., 2010. Dual boundary integral equation formulation in plane elasticity using complex variable. Eng. Anal. Boun. Elem. 34, 834–844.
Chen, Y.Z., Wang, Z.X., 2010. Dual boundary integral equation formulation in antiplane elasticity using complex variable. Comput. Mech. 45, 167–178.
Chen, Y.Z., Wang, Z.X., 2011. Solution for hole problems of elastic half-plane with gravity force using boundary integral equation. Int. J. Rock Mech. Mining Sci. 48, 520–526.
Chen, J.T., Wu, A.C., 2007. Null-field approach for the multi-inclusion problem under antiplane shears. ASME J. Appl. Mech. 74, 469–487.
Chen, J.T., Kuo, S.R., Lin, J.H., 2002. Analytical study and numerical experiments for degenerate scale problems in the boundary element method of two-dimensional elasticity. Int. J. Numer. Methods Eng. 54, 1669–1681.
Chen, Y.Z., Wang, Z.X., Lin, X.Y., 2009. A new kernel in BIE and the exterior boundary value problem in plane elasticity. Acta Mech. 206, 207–224.
Cheng, A.H.D., Cheng, D.S., 2005. Heritage and early history of the boundary element method. Eng. Anal. Boun. Elem. 29, 286–302.
Cruse, T.A., 1969. Numerical solutions in three-dimensional elastostatics. Int. J. Solids Struct. 5, 1259–1274.
Dong, C.Y., Lee, K.Y., 2005. A new integral equation formulation of two-dimensional inclusion–crack problems. Int. J. Solids Struct. 42, 5010–5020.
Dong, C.Y., Lo, S.H., Cheung, Y.K., 2002. Application of the boundary-domain integral equation in elastic inclusion problems. Eng. Anal. Bound. Elem. 26, 471–477.
Dong, C.Y., Lo, S.H., Cheung, Y.K., 2004. Numerical solution for elastic half-plane inclusion problems by different integral equation approaches. Eng. Anal. Bound. Elem. 28, 123–130.
Hong, H.K., Chen, J.T., 1988. Derivations of integral equations of elasticity. J. Eng. Mech. 114, 1028–1044.
Jaswon, M.A., Symm, G.T., 1977. Integral Equation Methods in Potential Theory and Elastostatics. Academic Press, London.
Kolte, R., Ye, W., Hui, C.Y., Mukherjee, S., 1996. Complex variable formulations for usual and hypersingular integral equations for potential problems—with applications to corners and cracks. Comput. Mech. 17, 279–286.
Legros, B., Mogilevskaya, S.G., Crouch, S.L., 2004. A boundary integral method for multiple circular inclusions in an elastic half-plane. Eng. Anal. Bound. Elem. 28, 1083–1098.
Linkov, A.M., 2002. Boundary Integral Equations in Elasticity. Kluwer, Dordrecht.
Luo, J.C., Gao, C.F., 2009. Faber series method for plane problems of an arbitrarily shaped inclusion. Acta. Mech. 208, 133–145.
Mogilevskaya, S.G., 2000. Complex hypersingular integral equation for the piecewise homogeneous half-plane with cracks. Int. J. Fract. 102, 177–204.
Mogilevskaya, S.G., Linkov, A.M., 1998. Complex fundamental solutions and complex variables boundary element method in elasticity. Comput. Mech. 22, 88–92.
Noda, N.A., Matsuo, T., 1998. Singular integral equation method for interaction between elliptical inclusions. ASME J. Appl. Mech. 65, 310–319.
Noda, N.A., Matsuo, T., 2000. Stress analysis of arbitrarily distributed elliptical inclusions under longitudinal shear loading. Int. J. Fract. 106, 81–93.
Rizzo, F.J., 1967. An integral equation approach to boundary value problems in classical elastostatics. Quart. J. Appl. Math. 25, 83–95.
Vodicka, R., Mantic, V., 2004. On invertibility of elastic single-layer potential operator. J. Elast. 74, 147–173.
Vodicka, R., Mantic, V., 2008. On solvability of a boundary integral equation of the first kind for Dirichlet boundary value problems in plane elasticity. Comput. Mech. 41, 817–826.